acoustics

MDPI

Article

Underwater Small Target Detection Method Based on the Short-Time Fourier Transform and the Improved Permutation Entropy

Jing Zhou [1,2], Baoan Hao [2], Yaan Li [1,*] and Xiangfeng Yang [2]

[1] School of Marine Science and Technology, Northwestern Polytechnical University, Xi'an 710072, China; zhoujing705@mail.nwpu.edu.cn
[2] Xi'an Precision Machinery Research Institute, National Key Laboratory of Underwater Information and Control, Xi'an 710077, China; baoanhao705@163.com (B.H.)
* Correspondence: liyaan@nwpu.edu.cn; Tel.: +86-29-8849-5817

Abstract: In the realm of underwater active target detection, the presence of reverberation is an important factor that significantly impacts the efficacy of detection. This article introduces the improved permutation entropy algorithm into the analysis of active underwater acoustic signals. Based on the significant difference between the improved permutation entropy in the frequency domain and the time domain, a frequency-domain-improved permutation entropy detection algorithm is proposed. The performance of this algorithm and the energy detection algorithm are compared and analyzed under the same conditions. The results show that the spectral entropy detector is about 2.7 dB better than the energy detector, realized via active small target signal detection under a reverberation background. At the same time, based on the characteristics of improved permutation entropy changing with the length of processed data, the short-time Fourier transform is integrated into frequency domain entropy detection to obtain distance and velocity information of the target. To validate the proposed methods, comparative analysis experiments were executed utilizing actual experiment data. The outcomes of both simulation and actual experiment data processing demonstrated that the sliding entropy feature detection method for signal spectrum has a small computational complexity and can quickly determine whether there is a target echo in the receive data. The two-dimensional entropy feature detection method for short-time signal spectra was found to effectively mitigate the impact of reverberation intensity and while enhancing the prominence of the target signal, thereby yielding a more robust detection outcome.

Keywords: improved permutation entropy; reverberation; underwater small target; nonlinear characteristics

Citation: Zhou, J.; Hao, B.; Li, Y.; Yang, X. Underwater Small Target Detection Method Based on the Short-Time Fourier Transform and the Improved Permutation Entropy. *Acoustics* **2024**, *6*, 870–884. https://doi.org/10.3390/acoustics6040048

Academic Editors: Yat Sze Choy and Jian Kang

Received: 21 August 2024
Revised: 25 September 2024
Accepted: 8 October 2024
Published: 10 October 2024

1. Introduction

Underwater acoustics is a discipline dedicated to the study of the behavior of sound waves as they propagate, reflect, scatter, and interact with submerged objects. The processing of underwater acoustic signals entails the extraction of meaningful information from a complex aquatic milieu. Amidst escalating global interest in the capabilities of underwater offense and defense, the detection of underwater targets has assumed a heightened significance. As global attention towards underwater offensive and defensive capabilities intensifies, the development and deployment of unmanned underwater vehicles, torpedoes, and other small underwater weapons have witnessed rapid growth. Due to their minute physical dimensions and exceptional concealment capabilities, underwater small targets pose a significant threat to ships and submarines [1–3]. To effectively counter these underwater small targets, ships must promptly detect threatening underwater targets and swiftly adopt defensive measures as soon as possible to improve the survival probability of

the ship. Consequently, the detection of underwater small targets is of great significance for the defense of ships and other vessels.

Due to the influence of random, time-variant, space-variant, and non-uniform ocean transmission, active echo signals exhibit strong distortion and nonlinear fluctuations [1]. Traditional nonlinear feature extraction methods for time series encompass Lyapunov exponents and fractal dimensions, etc. [4,5]. These methods are conceptually complex, computationally intensive, and require manual setting of numerous parameters during computation, which does not meet the requirements of real-time and intelligent processing for underwater acoustic detection systems. Information entropy theory, an essential branch of nonlinear theory, was introduced by Shannon into the field of communication, where he proposed the concept of information entropy [6]. Information entropy is a physical quantity that describes the amount of information in a system. The higher the order of the system, the smaller its information entropy value, and the greater the information content; conversely, the more disordered the system, the larger its information entropy value, and the smaller the information content. Information entropy algorithms have been widely used in human brain signal processing [7], fault diagnosis [8], animal recognition [9], disaster prediction, and other fields. Liu Lei and others have verified that multi-scale sample entropy can obtain more underwater target acoustic signal information than single-scale sample entropy [10]. Yuxing Li and others combined empirical mode decomposition with sample entropy, proving that this method can be applied to the feature extraction of ship radiation noise [11]. Chen Zhe empirical mode decomposition with multi-scale permutation entropy to classify the radiation noise of various ships [12]. Y Liang investigated the use of entropy-based techniques to achieve automatic detection of marine mammal tonal calls in passive acoustic monitoring data [13].

In the realm of underwater acoustic signal analysis, the approach that utilizes entropy information as a criterion for categorizing various ship-radiated noise types falls short in capturing the temporal and frequency characteristics for detecting target signals. This limitation renders such an approach unsuitable for the direct detection of underwater active signals. Within the scope of underwater active target signal detection, which is inherently complex due to the presence of reverberation, the application of entropy mainly involves calculating the entropy value for the feature vector extracted by traditional feature extraction methods, combining information entropy with existing feature extraction methods for underwater acoustic signal detection.

Currently, several typical information entropies [14–19] can analyze signal sequences, but there are still many shortcomings, such as the large computational load of the sample entropy algorithm, which is difficult to meet the requirements of real-time processing [20,21]; and permutation entropy, despite its utility, neglects the amplitude information of signals, resulting in a reduced ability to discriminate between different signals—a point emphasized in references [22–24].

In 2019, Chen et al. proposed an improved permutation entropy (IPE) algorithm [25], which not only enhances signal discrimination ability but also reduces the computational complexity of the algorithm. Compared with traditional information entropy algorithms, the IPE algorithm absorbs the advantages of the sample entropy algorithm, takes into account the signal amplitude and order information, and has good anti-noise performance. This paper introduces the improved permutation entropy algorithm (IPE) into the research of underwater active small target signal detection, proposing an underwater small target active signal detection method based on STFT-IPE. This method utilizes the strong signal discrimination ability of IPE, combined with the characteristics of STFT, to complete the nonlinear feature extraction and detection work of the active echo signal.

2. Materials and Methods

2.1. Spatiotemporal Reverberation Model

Reverberation is essentially the superposition of signals from scattering elements, and the method of superimposing the echo sequences of scattering elements to generate

reverberation data can reflect many characteristics of reverberation, such as spatiotemporal features. With the continuous research of spatiotemporal adaptive processing data processing methods, spatiotemporal adaptive methods can better fit the reverberation characteristics in the actual ocean caused by the motion of the sonar platform, which has caused the Doppler shift phenomenon of reverberation [26]. Jaffer and H. Cox have applied spatiotemporal reverberation models to underwater target detection research, which has better practical significance and application value [27,28].

Considering the random motion of scattering elements and adding the corresponding amplitude and phase modulation factors, the received reverberation sequence is:

$$\begin{aligned} s(t) &= \sum_{j=1}^{N_r} s_j(t) \\ &= \sum_{j=1}^{N_r} A_j(t) P_j(\omega) s_m\left[(1+d_{rj})t - \tau_j\right] \end{aligned}, \tag{1}$$

where N_r is the number of scattering elements contributing to the reverberation; $A_j(t)$ are random amplitude and phase modulation signals, reflecting the degree of random fluctuation of the scattering elements. P_j is the echo amplitude of the j-th scattering element, which is related to the transmitted signal strength, the scattering strength, and area represented by the scattering element, the beam directivity of transmission and reception, propagation expansion attenuation, and seawater absorption. $d_{rj} = 2v_s \cos\theta_j / c$ is the Doppler spread factor caused by the motion of the array element, v_s is the velocity of the receiving transducer, θ_j is the angle between the direction of the receiving transducer's velocity and the scattering element j, c is the speed of sound, and $\tau_j = 2r_j/c$ is the time delay of the transmitted signal after being scattered by the j-th scattering element to the array element, r_j is the distance between the receiving transducer and the j-th scattering element.

The ocean environment is set as a shallow sea with a depth of 100 m, with a sea state of three, and the seabed sediment is set to mud sediment. The sampling and transmission are combined to receive the transmitted signal. The transducer is submerged to a depth of 10 m, the platform speed is 50 knots, the transmitted signal is a CW signal with a frequency of 5000 Hz, and the transmission pulse width is 200 ms. The intensity of scattered echoes can be calculated based on sea surface conditions and seabed categories, and random amplitude and phase modulation can be added to the calculation. According to Formula (1) and parameter settings, the simulated reverberation signal is shown in Figure 1a, and the normalized reverberation signal is shown in Figure 1b. The echo signal is added with a time of 1 s, the target and platform radial motion speed is set to 75 knots, the signal-to-noise ratio (SNR) is 10 dB, and no background noise is added. The reverberation signal after adding the target echo signal and time-frequency diagram are shown in Figure 1c,d.

2.2. The Improved Permutation Entropy Algorithm

The improved permutation entropy algorithm (IPE) improves upon the traditional permutation entropy algorithm (PE) by addressing the issue of missing amplitude information [28]. This algorithm is capable of extracting more information from complex sequences while reducing computational complexity and enhancing signal resolution. The algorithmic flow is as follows:

(1) Normalize the time series $\{x_1, x_2, \cdots, x_N\}$ through the cumulative distribution function shown in the following equation. Where, μ and σ^2 represent the mean and variance of the time series, respectively.

$$y_i = \frac{1}{\sigma\sqrt{2\pi}} \int_{-\infty}^{x_i} e^{\frac{-(t-\mu)^2}{2\sigma^2}} dt, \tag{2}$$

(2) Phase space reconstruction, where, τ represent represents time delay:

$$Y_i = \left[y_i, y_{i+\tau}, \cdots, y_{i+(m-1)\tau}\right]_{1 \le i \le N-m+1}, \tag{3}$$

(3) Symbolize the first column $Y(:,1)$ of the phase space Y using the Uniform Quantification Operator (UQO) and calculate the corresponding symbolization result for the first column $S(:,1)$ of the phase space S.

$$UQO(u) = \begin{cases} 0 & y_{\min} \le u \le \Delta + y_{\min} \\ 1 & y_{\min} + \Delta \le u \le 2\Delta +_{\min} \\ \vdots & \vdots \\ L-1 & y_{\max} - \Delta \le u \le y_{\min}\ , \end{cases} \tag{4}$$

Here, L denotes a predetermined discretization parameter, Δ represents the discrete interval and meets $\Delta = (y_{\max} - y_{\min})/L$, $y_{\max}$ and $y_{\min}$ represent the maximum and minimum values of the subsequence y, respectively.

(4) The corresponding symbolization result $S(:,k)$ for the k column $Y(:,k)$ $(2 \le k \le m)$ of the phase space Y is obtained using the following formula,

$$S(j,k) = S(j,1) + floor[(Y(j,k) - Y(j,1))/\Delta]_{1 \le i \le N-\mathrm{m}+1}, \tag{5}$$

where floor indicates rounding down.

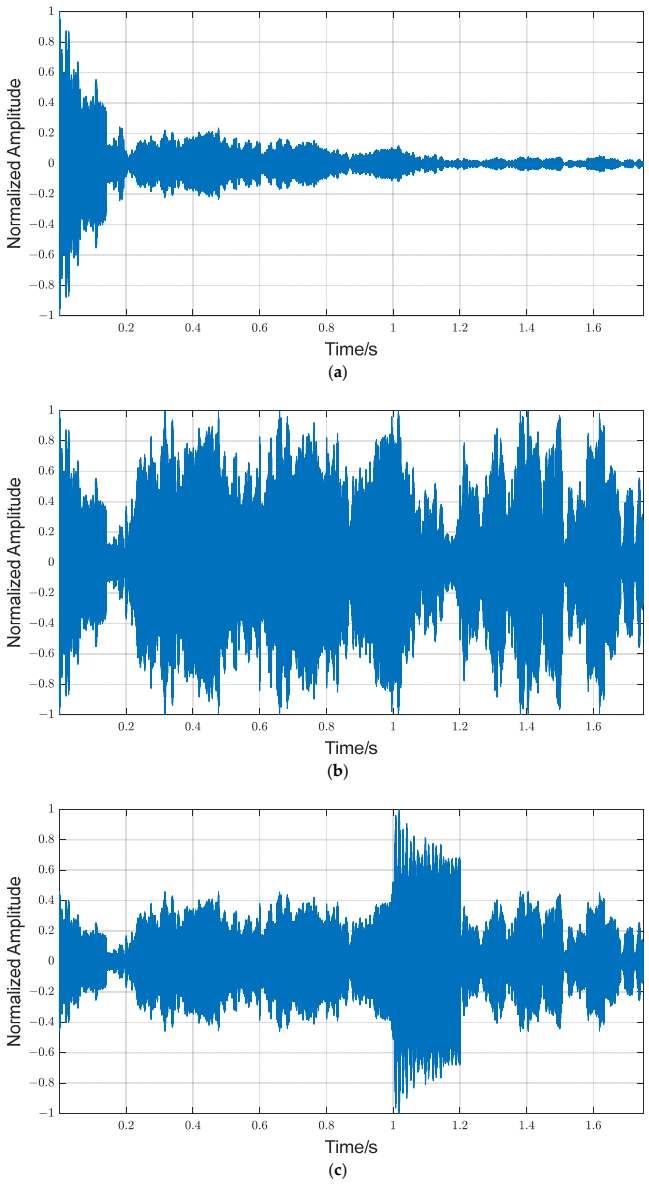

Figure 1. *Cont.*

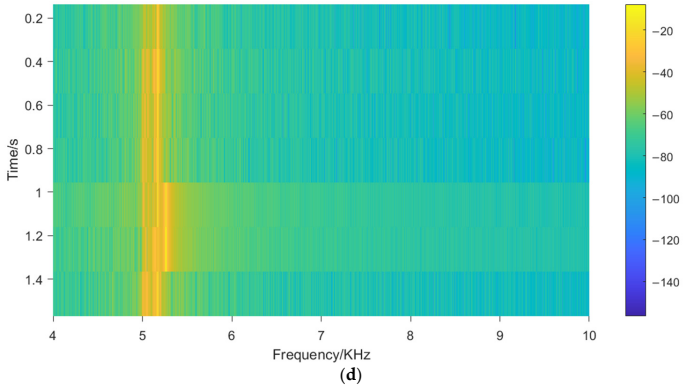

Figure 1. Simulation results of reverberation and target echo signals. (**a**) Reverberation signal; (**b**) normalized reverberation signal; (**c**) normalized reverberation signal after adding target echo signal; (**d**) time-frequency diagram of the target echo signal and reverberation.

IPE regards every row of the symbolized phase space S as a "pattern" $\pi_l, 1 \leq l \leq L^m$ and utilizes the term Symbol Pattern (SP) in the algorithm. Calculate the probability p_l of each SP in symbol phase space, according to the definition of Shannon entropy, the improved permutation entropy can finally be expressed as:

$$IPE(m, L) = -\sum_{l=1}^{L^m} p_l \ln p_l, \tag{6}$$

when only one element in the probability distribution of SP is 1 and the other elements are 0, IPE takes the minimum value 0. When the probability distribution follows a uniform distribution, IPE takes the maximum value $\ln(L^m)$. Therefore, IPE can be normalized. In this paper, normalized entropy values are used.

After normalizing Equation (6), we obtain:

$$\overline{IPE(m, L)} = IPE(m, L)/\ln(L^m), \tag{7}$$

The value of $\overline{IPE(m, L)}$ reflects the randomness of the time series. A larger choice of the discretization parameter L makes it more sensitive to noise fluctuations, while a smaller value of L can reduce the interference of noise to some extent.

2.3. Noise Variation Characteristics of Improved Permutation Entropy

The objective of this study is to investigate the sensitivity of IPE to noise. The discretization parameter L was set to 10, with an embedding dimension m of 3, a time delay τ of 1, and a data length N of 1000. The variations in both IPE and permutation entropy (PE) were examined. Simulations were conducted to generate 1000 sets of noise with normalized bandwidth ranging from 0.1 to 0.8. The entropy values and variance calculations in the time domain are presented in Figure 2 and Table 1, while those in the frequency domain are shown in Figure 3 and Table 2. The center of the error bars represents the average entropy value across 1000 trials, with the error bars indicating the standard deviation of the results. The short error bars for both entropy measures suggest a high degree of consistency in the estimation outcomes. As the bandwidth increases from narrow to wide, the changes in IPE in both the time and frequency domains are more pronounced than those in PE. Furthermore, IPE exhibits a more significant difference in the frequency domain compared to the time domain, indicating a heightened sensitivity of IPE to variations in noise signals. The standard deviation of IPE is larger than that of PE, which also indicates that the IPE method is more sensitive to noise signals due to considering the amplitude characteristics of the signal.

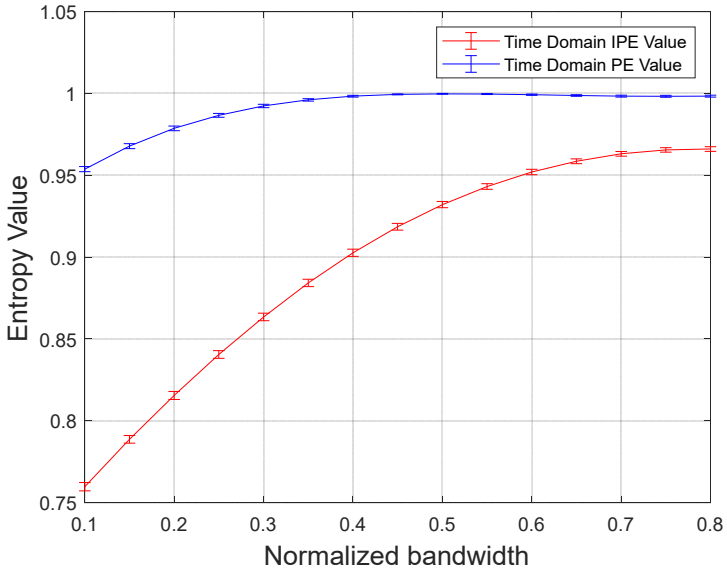

Figure 2. IPE and PE values of noise with different bandwidths in the time domain.

Table 1. IPE and PE values and variances of noise with different bandwidths in the time domain.

Normalized Bandwidth	0.1	0.2	0.3	0.4	0.5	0.6	0.7	0.8
IPE average value	0.966	0.9631	0.952	0.932	0.9026	0.8634	0.8155	0.7597
PE average value	0.9983	0.9983	0.9992	0.9997	0.9983	0.9923	0.9786	0.9537
IPE standard deviation	0.0014	0.0014	0.0016	0.0019	0.0021	0.0022	0.0023	0.0025
PE standard deviation	0.0006	0.0006	0.0004	0.0002	0.0005	0.0010	0.0014	0.0016

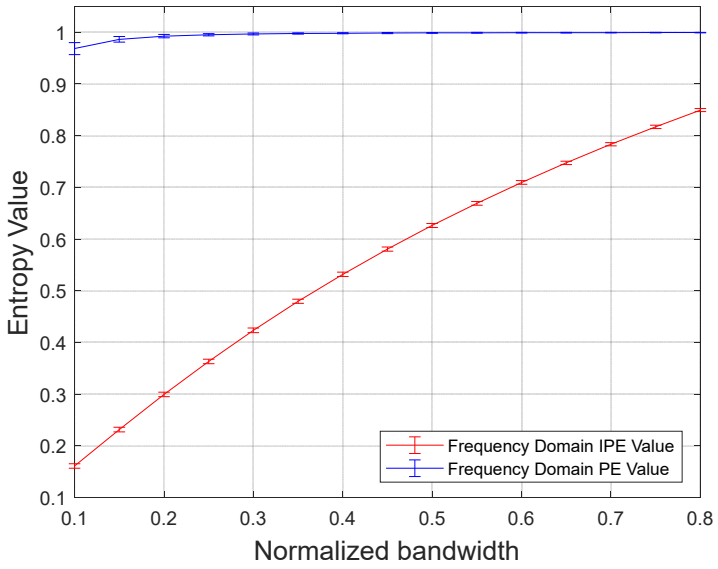

Figure 3. IPE and PE values of noise with different bandwidths in the frequency domain.

Table 2. IPE and PE values and variances of noise with different bandwidths in the frequency domain.

Normalized Bandwidth	0.1	0.2	0.3	0.4	0.5	0.6	0.7	0.8
IPE average value	0.8493	0.7833	0.7093	0.6262	0.5317	0.4233	0.2994	0.1611
PE average value	0.9993	0.9992	0.999	0.9986	0.998	0.9965	0.9923	0.9684
IPE standard deviation	0.0029	0.0031	0.0035	0.0038	0.0040	0.0044	0.0044	0.0043
PE standard deviation	0.0005	0.0006	0.0007	0.0008	0.0012	0.0017	0.0032	0.0115

3. Results

3.1. Detection Principle

The IPE is employed to quantify the complexity and sensitivity of the received signal in the frequency domain. By leveraging the differences in frequency domain uncertainty between the target echo pulse signal and the background and reverberation, the frequency domain entropy features are extracted to achieve signal detection. The detection of the echo signal is regarded as a hypothesis-testing problem, as shown in Equation (8):

$$\begin{cases} H_0: & x(n) = r(n) + w(n) \\ H_1: & x(n) = s(n) + r(n) + w(n)' \end{cases} \tag{8}$$

In the equations, $x(n)$ represents the received data, $s(n)$ is the signal, $r(n)$ is the reverberation, and $w(n)$ is the noise. H_0 indicates the situation where only reverberation and noise are received while H_1 indicates the situation where the received signal includes the target. The purpose of signal detection is to distinguish between these two different conditions and detect the target information.

3.2. Analysis of Spectral Entropy Detection Performance

The transmitted pulse width is set to 20 ms, the transmitted signal frequency to 5 kHz, and the received signal duration to 400 ms. The signal-to-noise ratio (SNR) is set from −12 dB to 2 dB. Figure 4 shows a performance comparison between two detection methods under the same detection threshold calculation criteria. It can be observed that when the detection probability d is 0.5, the spectral entropy detector has an SNR of approximately −6 dB, which is 2.7 dB better than the energy detector.

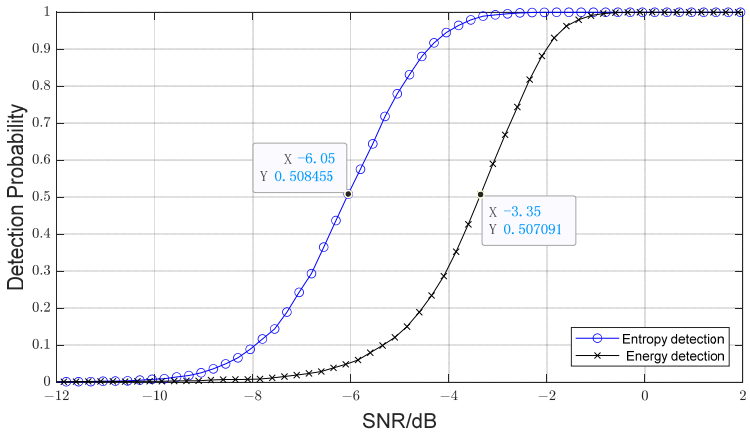

Figure 4. Spectral entropy detection and energy detection performance curve.

To investigate the impact of data length on detection effectiveness, the transmitted pulse width is set to 20 ms, the transmitted signal frequency to 5 kHz, and the SNR to −5 dB. The received signal duration varies from 80 ms to 1000 ms. Figure 5 shows the variation in spectral entropy detection performance with data time length under different SNR conditions. It can be seen that when the data time length is between 0.2 s and 0.4 s, the detection probability is significantly higher than at other durations.

For active target signal detection, sliding segment processing is applied to the data of the active period, followed by entropy detection, which can better utilize the advantages of entropy detection. Sliding segment processing is similar to the characteristics of the short-time Fourier transform (STFT); therefore, by combining the features of STFT and entropy detection, an appropriate sliding window can be selected for the spectral entropy detection algorithm. This not only detects the target but also provides information about the target's velocity and distance, forming an active detection algorithm based on STFT-IPE.

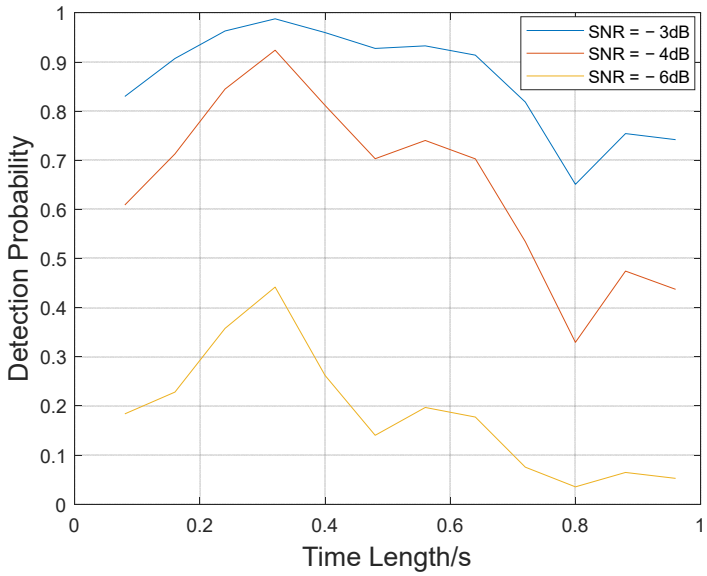

Figure 5. Variation of spectral entropy detection performance with data time length under different SNR conditions.

4. Discussion

4.1. Simulation Signal Data Verification

Utilizing the reverberation signal simulation results from the space-time model in Section 1, this study examines the entropy characteristics of data after adding target echo signals and background noise of varying intensities to the received reverberation signals. The influence of noise and reverberation on the performance of the entropy feature detection algorithm is investigated.

4.1.1. Improved Permutation Entropy Detection Algorithm under Reverberation Background

At the end of an active detection cycle, a preliminary judgment is made on the presence or absence of detection targets within the cycle. Therefore, the entire cycle signal is selected for IPE detection calculation. Assuming a moving small target's relative velocity to the sonar platform is 75 knots, after adding target signals and noise of different intensities to the reverberation simulation signal, the spectral entropy of the simulation signal is calculated. A sliding window is applied to the spectral signal, and the IPE of each window's spectral sequence is calculated. A short-time Fourier transform (STFT) is then performed on the improved permutation entropy sequence to obtain a pseudo-time-frequency diagram of the IPE. The entropy characteristics of the signal spectrum under different signal-to-noise ratio (SNR) and signal-to-reverberation ratio (SRR) conditions are analyzed based on the processing results.

(1) Under the reverberation background, target signals and background noise are added to achieve an SRR of 5 dB and an SNR of 0 dB. The simulation results are shown in Figure 6.

From Figure 6, it is evident that reverberation and target signals can be distinctly differentiated, proving that the algorithm can be applied to target signal detection under noisy conditions.

(2) Under the reverberation background, target signals and background noise are added to achieve an SRR of 5 dB and an SNR of −15 dB. The simulation results are shown in Figure 7.

From Figure 7a, it can be observed that the IPE algorithm struggles to effectively detect the target signal under conditions of excessively low SNR, where the entropy features are completely submerged in the noise environment, making it impossible to distinguish between target signals and noise.

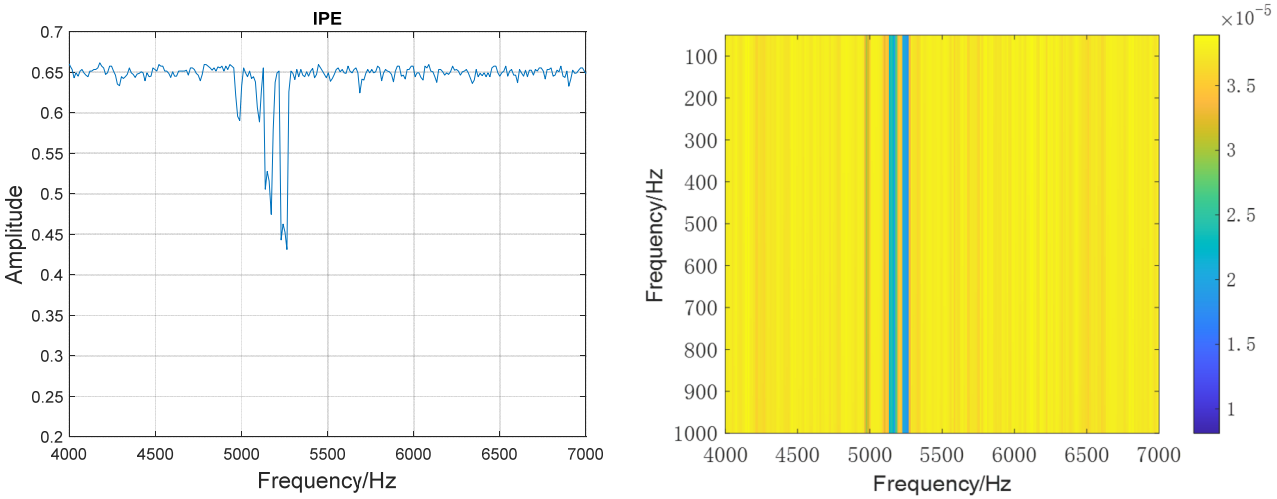

Figure 6. IPE result of the signal spectrum when the signal-to-noise ratio is 0 dB. (**a**) IPE value of the spectrum under a sliding window; (**b**) STFT for IPE value.

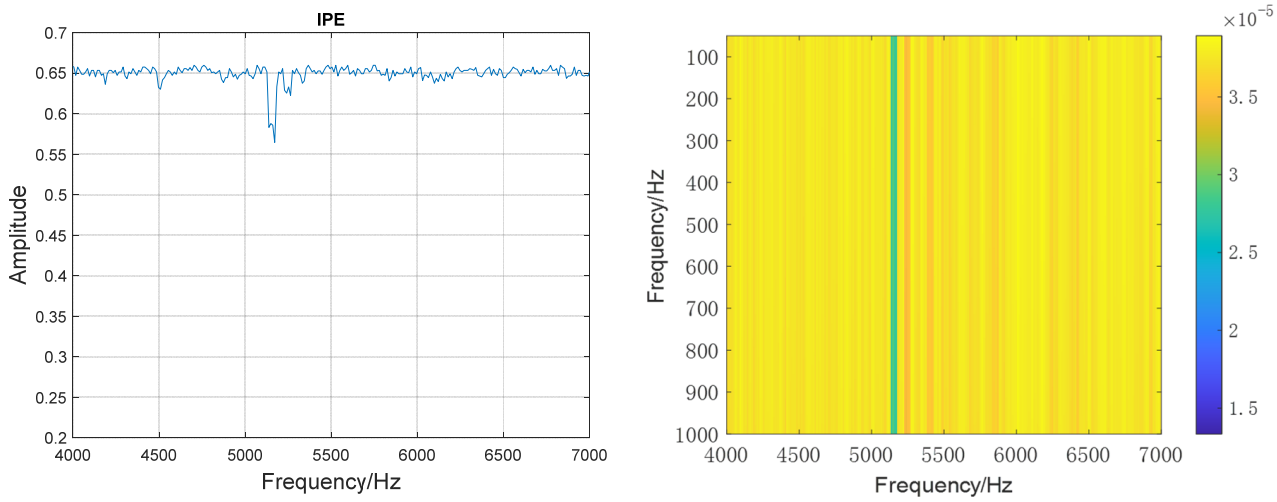

Figure 7. IPE result of the signal spectrum when the signal-to-noise ratio is −15 dB. (**a**) IPE value of the spectrum under a sliding window; (**b**) STFT for IPE value.

4.1.2. STFT-IPE Active Detection Algorithm under Reverberation Background

After the preliminary judgment is completed, a detailed analysis is conducted on the active cycle that may contain target signals. The sliding window method is employed, and the STFT-IPE active detection algorithm is used to detect signals within the cycle, determining the time and frequency information of the target.

(1) Only Gaussian white noise is added to the simulated reverberation signal. The time-frequency analysis diagram of the signal is shown in Figure 8, and the entropy features of the power spectrum at different time and frequency frames are shown in Figure 9.

From Figure 9, it can be seen that there are no significant peaks in the entropy features of the power spectrum at the time frame, and there are only minor fluctuations at the reverberation frequency in the frequency frame, with no significant peaks. In the time-frequency diagram, there are clear peaks due to reverberation, while in the frequency domain entropy, there are only minor fluctuations. Therefore, entropy feature detection in the frequency domain can effectively resist the interference caused by reverberation, thereby suppressing reverberation.

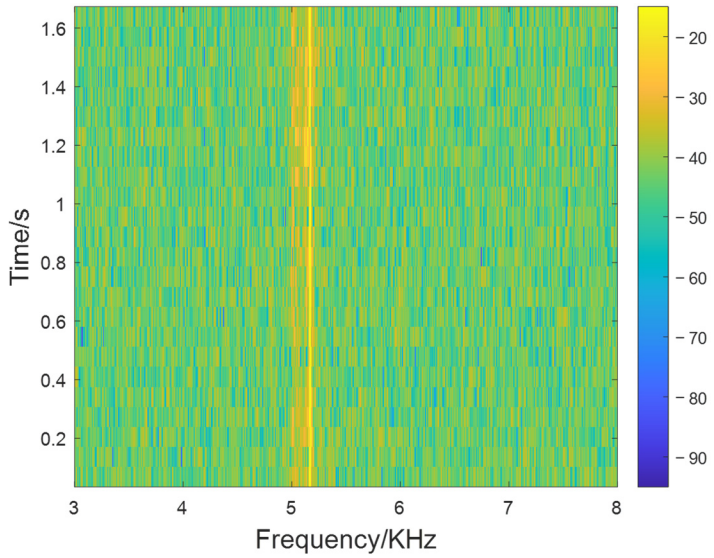

Figure 8. The time-frequency analysis diagram of reverberation with noise.

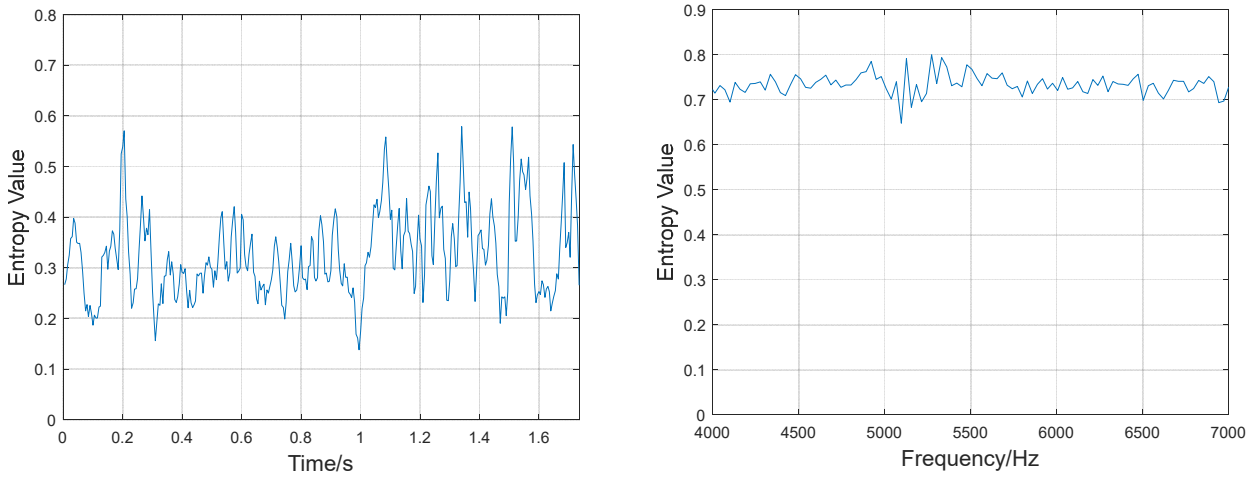

Figure 9. Entropy characteristics of the power spectrum in different time and frequency frames when only Gaussian white noise is added. (**a**) Entropy characteristics of the power spectrum in time frames; (**b**) entropy characteristics of the power spectrum in frequency frames.

(2) Under the reverberation background, noise and signals are added to achieve an SNR of 0 dB. The entropy characteristics of the power spectrum in different time and frequency frames are shown in Figure 10.

From Figure 10a, it can be observed that there are significant continuous changes in the entropy value of the power spectrum at the time frame within the time range of the target echo. From Figure 10b, it can be seen that there is a clear peak in the frequency range of the target echo when a target is present. Applying the IPE algorithm to the short-time power spectrum of the signal can effectively detect the time and frequency of the target signal and suppress the reverberation signal characteristics while highlighting the target signal characteristics.

Through simulation signal verification, it can be seen that the sliding entropy feature detection method for time series can detect the frequency of the target, and the computational load is small, making it suitable for rapid judgment of whether there is a target echo in the echo. The STFT-IPE based active detection algorithm can detect information such as the target's distance and speed, and the frequency detection can suppress the intensity of reverberation and highlight the target signal, making the effect more robust.

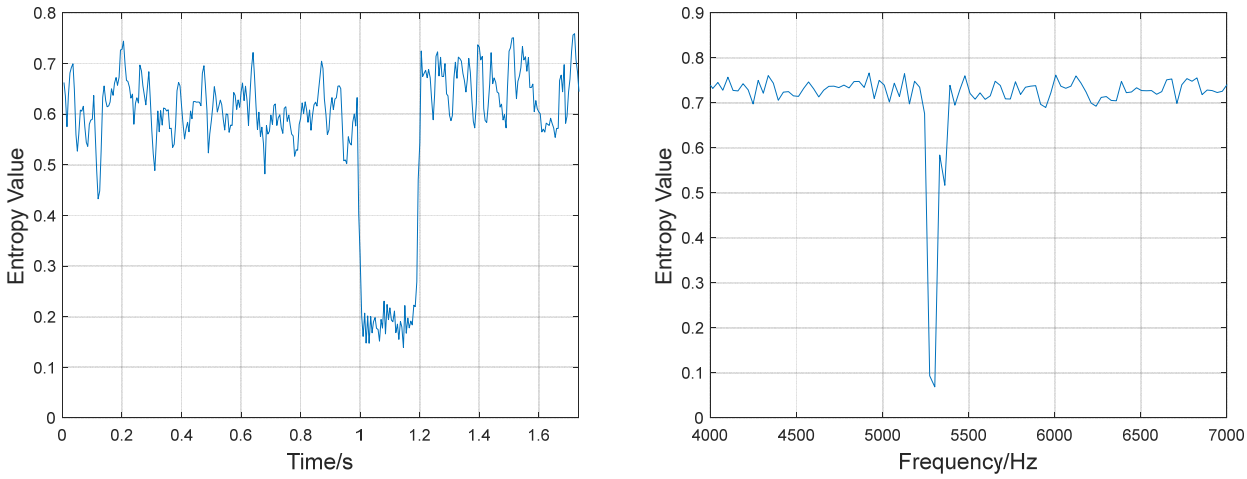

(**a**) (**b**)

Figure 10. Entropy characteristics of the power spectrum in different time and frequency frames when the signal-to-noise ratio is 0 dB. (**a**) Entropy characteristics of the power spectrum in time frames; (**b**) entropy characteristics of the power spectrum in frequency frames.

4.2. Experimental Data Verification

Data collected from the actual experiment is selected for verification. The active sonar signal is a CW signal with a transmission pulse width of 50 ms and an active cycle duration of 600 ms.

4.2.1. Comparison and Validation of Experimental Data with and without Targets

To compare the target detection effects, two sets of data are processed: one without targets in the cycle and the other with target echoes in the cycle. When there is a target, the platform is approximately 350 m from the target. After excluding the transmission and control time within the working cycle, the active acquisition of time-domain waveforms and time-frequency maps are shown in Figures 11 and 12. Comparing Figures 11 and 12, it can be seen that the data with target signals clearly have bright lines.

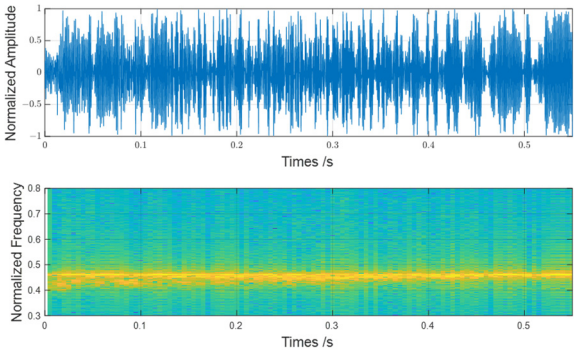

Figure 11. Active acquisition of time-domain waveforms and time-frequency maps without target signals.

Analyzing the active sampling data without target signals, the entropy feature detection results of the time frame and frequency frame are shown in Figure 13. The IPE value of the power spectrum at the time frame has a clear peak at 0.1 s, which is analyzed to be due to reverberation extension. The IPE value of the power spectrum at the frequency frame fluctuates within the reverberation frequency range and is relatively uniform in other frequency bands. Combining the results of the time frame and frequency frame, it can be judged that there is no target.

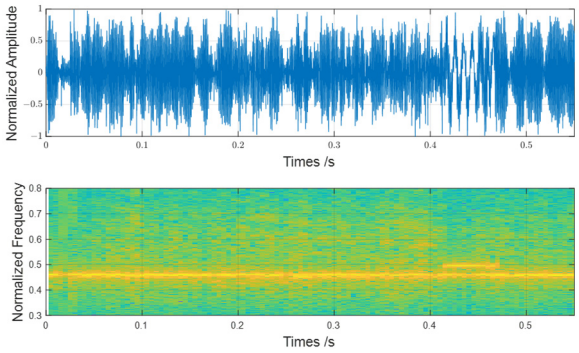

Figure 12. Active acquisition of time-domain waveforms and time-frequency maps when there is a target signal.

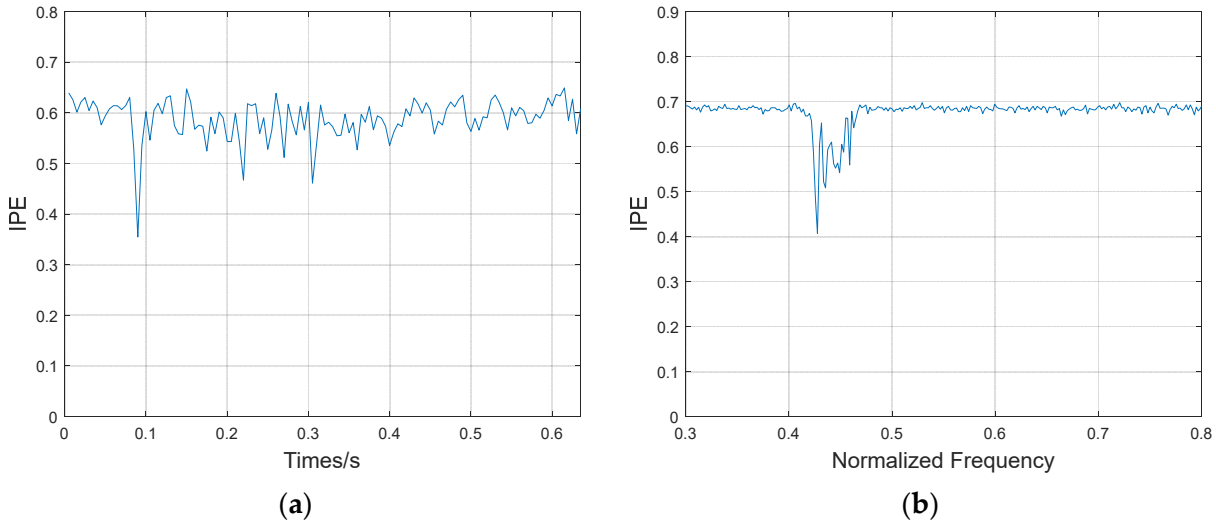

Figure 13. Detection result without target signal. (**a**) Entropy characteristics of the power spectrum in time frames; (**b**) entropy characteristics of the power spectrum in frequency frames.

Analyzing the active sampling data with target signals, the entropy feature detection results of the time frame and frequency frame are shown in Figure 14. The improved permutation entropy of the power spectrum at the time frame has a clear peak at 0.445 s, consistent with the appearance of the target. The IPE of the power spectrum at the frequency frame, apart from minor fluctuations at the reverberation position, has a clear peak at the normalized frequency of 0.4941.

Comparing Figures 13 and 14, it can be seen that when there is no target, the entropy feature at the time frame has significant fluctuations near 0.1 s, and the entropy feature in the frequency frame fluctuates within the reverberation frequency range, with no significant fluctuations in other frequency bands. Combining the results of the time frame and frequency frame processing, it can be judged that there is no target appearance. Selecting the cycle data with target signals for analysis, the results are shown in Figure 14. The IPE value of the power spectrum at the time frame has a clear peak at 0.445 s, due to the absence of amplitude modulation of the target echo in the simulation signal, and the echo amplitude in the actual experimental is not an ideal CW signal due to the influence of channels and other factors. Therefore, in the actual experimental data time frame processing results, there is no continuous low entropy value feature as in the simulation signal processing results, only a lower peak can be seen. Here, the zero moment of time is the start of sampling, and after adding the transmission time and control time, it is basically consistent with the moment corresponding to the target distance. Apart from minor fluctuations at the reverberation position in the frequency frame power spectrum's IPE value, there is a clear peak at the normalized frequency of 0.4941. Combining the results of the time frame and

frequency frame, it can be judged that there is a target, and the target's distance and speed information can be obtained.

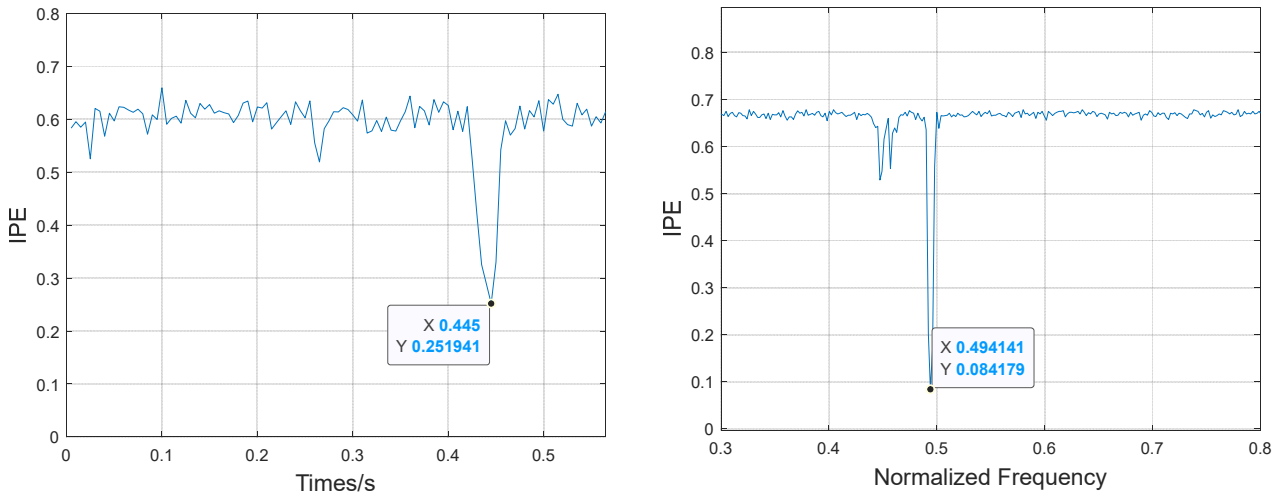

(**a**) (**b**)

Figure 14. Detection results with a target signal. (**a**) Entropy characteristics of the power spectrum in time frames; (**b**) entropy characteristics of the power spectrum in frequency frames.

4.2.2. Comparison of Experimental Data at Different Distances

To compare the effects of target detection at different distances and signal-to-noise ratios (SNRs), experimental data for target distances of 432 m, 349 m, and 292 m were analyzed. The entropy feature detection results obtained for time frames and frequency frames at different distances are illustrated in Figure 15. It is evident that as the proximity to the target increases, the entropy value peaks in the time frames occur increasingly earlier. In the frequency frames, the entropy values in the reverberation frequency bands exhibit a relatively stable trend across different distances, while the entropy values in the target frequency bands decrease progressively with decreasing distance. This trend corroborates the effectiveness of the small target detection algorithm based on the STFT-IPE in accurately detecting targets.

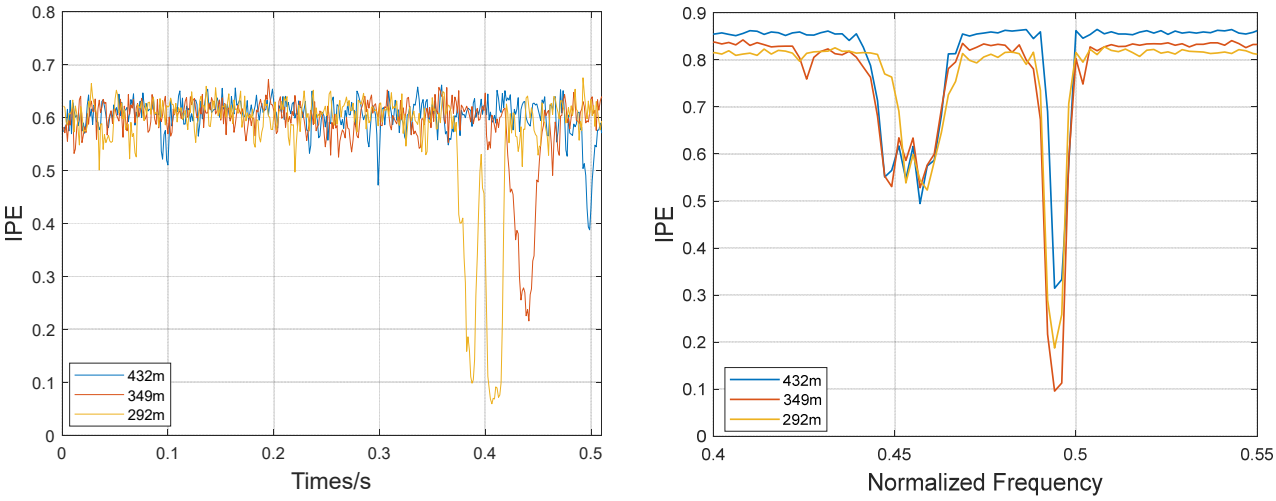

(**a**) (**b**)

Figure 15. Detection results for different distance targets. (**a**) Entropy characteristics of the power spectrum in time frames; (**b**) entropy characteristics of the power spectrum in frequency frames.

5. Conclusions

Based on the characteristic that IPE has more significant differences in the frequency domain than in the time domain, the IPE algorithm is introduced into active underwater signal analysis, proposing a frequency domain IPE detection algorithm. Under the same conditions, the spectral entropy-based detector outperforms the traditional energy detector by a margin of approximately 2.7 dB. This enhancement facilitates the reliable detection of active small target signals amidst a challenging reverberation background. Moreover, in light of the observation that IPE values are sensitive to the length of the processed data, STFT is introduced into the frequency domain entropy detection to obtain the target's distance and speed information. The robustness and efficacy of the proposed algorithm have been rigorously validated through a series of simulations and actual experiment data. Our findings demonstrate that the sliding window-based entropy feature detection method for signal spectra is computationally efficient and can swiftly ascertain the presence of target echoes within the acquired data. The two-dimensional entropy feature detection approach for the signal's short-time power spectrum effectively mitigates the impact of reverberation intensity while enhancing the salience of the target signal, thereby rendering the detection process more robust. The results show that the sliding entropy feature detection method for signal spectrum has a small computational load and can quickly determine whether there is a target echo in the received data. The two-dimensional entropy feature detection method for signal short-time power spectrum can suppress the intensity of reverberation and highlight the target signal, making the effect more robust.

The proposed method in this paper significantly enhances the detection capabilities of underwater targets, aiding naval vessels and submarines in promptly identifying and responding to potential threats within underwater operational environments. The swift and precise detection of enemy submarines or unmanned underwater vehicles (UUVs) is paramount for defensive strategies, thereby enhancing the survival capabilities of naval craft. Furthermore, in the context of marine ecological monitoring, this methodology can be harnessed to observe biological activities within the ocean, such as fish schooling and dolphin migrations, providing valuable insights for scientists to comprehend the dynamic changes within oceanic ecosystems. However, the present study focuses on underwater small-target signal detection without considering the characteristic variations of reverberation across diverse acoustic channels. For instance, a comparison of entropy characteristics of reverberation signals under varying underwater acoustic environmental conditions could offer insights into the impact of marine environments on reverberation complexity, warranting further investigation.

Author Contributions: J.Z.: conceptualization, methodology, software, writing—original draft, writing—review and editing, funding acquisition. B.H.: methodology, writing—original draft, writing—review and editing. Y.L.: methodology, writing—original draft, writing—review and editing, funding acquisition. X.Y.: methodology, writing—original draft, writing—review and editing. All authors have read and agreed to the published version of the manuscript.

Funding: This work is supported by the fund of National Key Laboratory of Underwater Information and Control.

Data Availability Statement: The datasets analyzed during the current study are available from the corresponding authors on reasonable request.

Conflicts of Interest: The authors declare no conflicts of interest.

References

1. Zhang, B. Status and development of the surface ship torpedo defense technology. *Tech. Acoust.* **2015**, *2*, 180–183.
2. Huang, H.; Li, Y. Underwater acoustic detection: Current Status and future trends. *Bull. Chin. Acad. Sci.* **2019**, *34*, 264–271.
3. Cui, G. Foreign anti-torpedo torpedo development and trend analysis. *Ship Sci. Technol.* **2013**, *35*, 138–141.
4. Yang, S.; Li, Z.; Wang, X. Ship recognition via its radiated sound: The fractal based approaches. *J. Acoust. Soc. Am.* **2002**, *112*, 172–177. [CrossRef]
5. Yang, S.; Li, Z. Classification of ship-radiated signals via chaotic features. *Electron. Lett.* **2003**, *39*, 395–397. [CrossRef]

6. Shannon, C. A mathematical theory of communication. *Bell Syst. Tech. J.* **1948**, *27*, 379–423. [CrossRef]
7. Yao, W.; Liu, T.; Dai, J.; Wang, J. Multiscale Permutation Entropy analysis of electroencephalogram. *Acta Phys. Sin.* **2014**, *7*, 427–433.
8. Han, M.; Pan, J. A fault diagnosis method combined with LMD, sample entropy and energy ratio for roller bearings. *Measurement* **2015**, *76*, 7–19. [CrossRef]
9. Nielsen, L.R.; Tervo, O.M.; Blackwell, S.B.; Heide-Jørgensen, M.P.; Ditlevsen, S. Using quantile regression and relative entropy to assess the period of anomalous behavior of marine mammals following tagging. *Ecol. Evol.* **2023**, *13*, e9967. [CrossRef]
10. Liu, L.; Bao, X.; Chen, X. A Study of surface vessel recognition based on multi-scale sample entropy. *J. Netw. New Media* **2014**, *3*, 28–31.
11. Li, Y.X.; Li, Y.; Chen, X. A Feature Extraction Method of Ship-Radiated Noise Based on Sample Entropy and Ensemble Empirical Mode Decomposition. *J. Unmanned Undersea Syst.* **2018**, *26*, 28–34.
12. Chen, Z.; Li, Y. A study on complexity feature extraction of ship radiated signals based on a multi-scale permutation entropy method. *J. Vib. Shock* **2019**, *38*, 225–230.
13. Liang, Y.; Kerri, D.; Nicholas, J. Entropy-Based Automatic Detection of Marine Mammal Tonal Calls. *IEEE J. Ocean. Eng.* **2024**, *9*, 1558–1691. [CrossRef]
14. Bandt, C.; Pompe, B. Permutation Entropy: A Natural Complexity Measure for Time Series. *Phys. Rev. Lett.* **2002**, *88*, 74–102. [CrossRef] [PubMed]
15. Aziz, W.; Arif, M. Multiscale Permutation Entropy of Physiological Time Series. In Proceedings of the IEEE 2005 Pakistan Section Multitopic Conference, Karachi, Pakistan, 24–25 December 2005.
16. Renyi, A. Title of the article on measures of information and entropy. In Proceedings of the 4th Berkeley Symposium on Mathematical Statistics and Probability, California, CA, USA, 20 June–30 July 1960; Volume 1961, pp. 547–561.
17. Pincus, S. Approximate entropy as a measure of system complexity. *Proc. Natl. Acad. Sci. USA* **1991**, *88*, 2297–2301. [CrossRef]
18. Bian, C.; Qin, C.; Ma, Q. Modified permutation-entropy analysis of heartbeat dynamics. *Phys. Rev. E* **2012**, *85*, 021906. [CrossRef]
19. He, S.; Sun, K.; Wang, H. Modified multiscale permutation entropy algorithm and its application for multiscroll chaotic systems. *Complexity* **2016**, *21*, 52–58.
20. Richman, J.; Moorman, J. Physiological Time-Series Analysis Using Approximate Entropy and Sample Entropy. *Acad. Am. J. Physiol. Heart Circ. Physiol.* **2000**, *278*, 39–49. [CrossRef]
21. George, M.; Md, A.; Roberto, S. Low Computational Cost for Sample Entropy. *Entropy* **2018**, *20*, 61. [CrossRef]
22. Zunino, L.; Olivares, F.; Scholkmann, F.; Rosso, O.A. Permutation entropy based time series analysis: Equalities in the input signal can lead to false conclusions. *Phys. Lett. A* **2017**, *381*, 1883–1892. [CrossRef]
23. Fadlallah, B.; Chen, B.; Keil, A. Weighted-permutation entropy: A complexity measure for time series incorporating amplitude information. *Phys. Rev. E Stattistical Nonlinear Soft Matter Phys.* **2013**, *87*, 022911. [CrossRef] [PubMed]
24. Cuesta–Frau, D.; Varela–Entrecanales, M.; Molina–Picó, A. Patterns with Equal Values in Permutation Entropy: Do They Really Matter for Biosignal Classification? *Complexity* **2018**, *2018*, 1324696. [CrossRef]
25. Chen, Z.; Li, Y.; Liang, H. Improved permutation entropy for measuring complexity of time series under noisy condition. *Complexity* **2019**, *2019*, 1403829. [CrossRef]
26. Zhan, H.; Cai, Z.; Yuan, B. Space-Time adaptive Reverberation Suppression in active sonar of torpedo. *J. Wuhan Univ. Technol.* **2007**, *31*, 947–950.
27. Jaffer, A.G. Constrained partially adaptive space-time processing for clutter suppression. In Proceedings of the 1994 28th Asilomar Conference on Signals, Systems and Computers, Pacific Grove, CA, USA, 31 October–2 November 1994.
28. Cox, H. Space-time processing for suppression of bottom reverberation. In Proceedings of the Conference on Signals, Systems & Computers, Pacific Grove, CA, USA, 30 October–1 November 1995.